Clinical Evaluation of the MIRA Technique in Cellulite Treatment: A Retrospective Case–Control Study

Dora Intagliata * and Maria Luisa Garo *

Posted Date: 11 March 2026

doi: 10.20944/preprints202603.0862.v1

Keywords: cellulite; intradermal injection; subcutaneous injection; ultrasound

 doi:10.20944/preprints202603.0862.v1

Article

Clinical Evaluation of the MIRA Technique in Cellulite Treatment: A Retrospective Case–Control Study

Dora Intagliata [1,*] and Maria Luisa Garo [2,*]

[1] Poliambulatorio ID Future, 96100 Siracusa, Italy

[2] Biostatistics and Research Methodology Unit, Mathsly Research, 89900 Vibo Valentia, Italy

* Correspondence: idmedicalsrl@gmail.com (D.I.) and marilu.garo@mathsly.it (M.L.G.)

Abstract

Background: Cellulite is a highly prevalent aesthetic concern characterized by structural remodeling of subcutaneous adipose tissue and fibrous septa, resulting in visible skin irregularities. Despite the availability of many injectable treatments with documented efficacy, most standard approaches adopt uniform protocols that overlook interindividual anatomical variability, potentially limiting treatment precision and clinical outcomes. This retrospective case–control study evaluated the Modulated Insertion of Regenerative Activation (MIRA), a technique that individualizes needle length and injection angle according to ultrasound findings, modulating insertion parameters to stimulate regenerative responses within dermal and subcutaneous layers. **Methods:** Clinical and ultrasonographic data from 120 women with stage 3 cellulite were analyzed. Stage 3a patients received carbon dioxide therapy (CDT), whereas stage 3b patients underwent injectable solution therapy (IST). Within each treatment, patients were allocated to MIRA or control groups. **Results**: Compared with controls, MIRA showed greater reductions in adipose tissue thickness (CDT: −1.6 mm; IST: −1.5 mm; p_{adj} = 0.002), nodules, pain, edema, and fibrosis, with improved fascia regularity. Patient satisfaction was higher in MIRA (CDT: 8.1 ± 1.6; IST: 8.5 ± 1.4; p_{adj} = 0.002), and over 76% reported improved skin quality. **Conclusion**: Ultrasound-guided modulation of needle parameters with MIRA may enhance structural and esthetic outcomes compared with standard approaches.

Keywords: cellulite; intradermal injection; subcutaneous injection; ultrasound

1. Introduction

Cellulite, medically referred to as edematous fibrosclerotic panniculopathy (EFP), is a common condition that affects approximately 85–98% of post-pubertal women[1,2]. Clinically, the disease manifests itself as an uneven skin surface, often described as "cottage cheese" or "orange peel" skin, which is due to structural changes in the subcutaneous fatty tissue and microcirculation[3–5].

The pathophysiology of cellulite is multifactorial and involves variations in the distribution of adipose tissue, skin texture and the integrity of the connective tissue septa[6,7]. Apart from its physical manifestations, cellulite can also have a significant impact on patients◎self-perception and quality of life. Therefore, accurate diagnosis and assessment are essential for the development of effective treatment strategies to ensure successful treatment for patients[8,9].

In this context, multimodal approaches combining injectable treatments and physical modalities have shown promising results in improving both the subjective and objective results of cellulite, with a reduction in the thickness of subcutaneous fat tissue and an improvement in skin profile documented on ultrasound images[10,11]. Injection-based approaches are widely used to improve skin texture and contour in areas affected by cellulite[12–15]. These approaches usually involve the introduction of customized mixtures of active ingredients aimed at promoting local lipolysis, improving lymphatic drainage and stimulating remodeling of the skin[16,17], or the delivery of

 doi:10.20944/preprints202603.0862.v1

carbon dioxide (CO_2) which improves microcirculation, oxygenation and collagen synthesis, ultimately leading to visible improvement in skin quality[18]. Despite their popularity, these procedures are often performed using standardized parameters for needle type and insertion angle without taking into account the inter-individual variability of septal architecture and adipose layer depth. This lack of personalization may limit therapeutic efficacy and contribute to heterogeneous clinical outcomes, especially in advanced stages of cellulite where the fibrous septa are particularly pronounced.

Over the years, high-frequency ultrasound has proven to be a valuable, non-invasive imaging technique that can be used to visualize the structural changes in subcutaneous tissue associated with cellulite[7,19,20]. A recent study by Intagliata et al. (2025) proposed a reproducible method for evaluating the morphology of advanced cellulite that allows detailed visualization of adipocyte clusters and the organization of fibrous septa. Such imaging can complement traditional clinical classification systems and allow for more precise and objective grading[21].

Beyond diagnostic purposes, ultrasound offers the possibility of supporting treatment planning. By mapping the density of the fibrous septa and measuring the exact tissue depth, ultrasound can influence the choice of needle and injection angle, thus increasing the precision of injection procedures. Although both injection techniques and ultrasound imaging are well documented in the treatment of cellulite, there is currently no standardized technique that integrates these two modalities into a unified, image-guided treatment strategy. Specifically, there is a lack of evidence-based guidelines that translate ultrasound-derived parameters into practical therapeutic decisions, such as the selection of optimal needle length and insertion angle tailored to the patient's unique subcutaneous anatomy.

The aim of this retrospective study is to validate a technique – called Modulated Insertion of Regenerative Activation (MIRA) – for cellulite treatment that uses pre-procedural ultrasound parameters to personalize both needle selection and insertion angle according to individual anatomical features.

2. Materials and Methods

Study Design and Participants

This retrospective case–control study evaluated the validity of the MIRA technique compared with the standard approach, which neglects individual anatomical variability, applying identical needle length and insertion angle parameters across all patients. Clinical and ultrasonographic data were retrospectively collected from medical records of procedures performed between January and July 2025 in a private clinical setting (Siracusa, Italy).

Patients were eligible for inclusion if they were women aged 18–55 years with stage 3 cellulite, as determined by the Nürnberger–Müller scale [22], and had complete baseline (T0) and follow-up (T1) data available. Exclusion criteria were: (1) Pregnancy or breastfeeding at the time of treatment; (2) Current or recent (<6 months) systemic corticosteroids, hormonal therapy, or weight-loss medications; (3) Prior aesthetic or surgical procedures in the thighs or gluteal region within the previous 12 months; (4) Relevant endocrine or metabolic disorders (e.g., uncontrolled diabetes, thyroid dysfunction, Cushing's syndrome); (5) Connective tissue or dermatological diseases interfering with outcome assessment; (6) Severe cardiovascular, hepatic, or renal disease; (7) Missing or incomplete follow-up data.

Cases were defined as patients treated with MIRA technique, while controls were selected among patients managed with standard care without MIRA technique and matched for age (±3 years) and BMI (±2 kg/m²).

Ethical Statement

The procedures applied in this study are part of routine clinical practice in aesthetic medicine and were performed exclusively with CE-marked medical devices used within their approved

 doi:10.20944/preprints202603.0862.v1

indications. The MIRA technique does not introduce new drugs, devices, or experimental interventions, but systematizes the selection of needle length and injection angle based on ultrasound imaging. According to Italian regulations (Ministerial Decree of 2 September 2002 and subsequent updates by AIFA), clinical activities that fall entirely within standard practice and involve CE-marked devices used as indicated are not classified as clinical trials. Accordingly, this study was classified as a methodological/quality improvement evaluation of routine clinical practice, with no use of investigational drugs or devices and no deviation from standard care pathways. The Clinical Medical Directorate where the study was conducted, formally issued a waiver from Ethics Committee review (Prot. 04/2024). The study was nonetheless conducted in accordance with the Declaration of Helsinki and the principles of Good Clinical Practice. All patients provided written informed consent for the anonymous use of their clinical and ultrasound data for research and publication purposes.

MIRA Technique

The MIRA technique was developed to close the gap between morphological ultrasound assessment of subcutaneous tissue and subsequent targeted therapeutic intervention. The basic idea is to individualize the treatment parameters, adapted to the ultrasound characteristics of the adipose tissue and superficial fascia according to the classification of the IEC system[21]. MIRA is a technique based on the controlled modulation of needle insertion parameters to induce regenerative responses within the dermal and subcutaneous compartments.

Unlike conventional injection protocols that rely solely on microtrauma-induced remodeling, it employs a strategic geometry of insertion designed to activate localized cellular signaling and structural reorganization processes.

Operatively, the MIRA technique aims to adapt the injection depth and angle to the specific ultrasound-based staging of the patient in order to optimize the delivery of the treatment to the intended target compartment and ensure homogeneous contact with the pathological substrate. This precise targeting facilitates the mobilization of interstitial fluid, improves lymphatic drainage, and attenuates local inflammation, all of which contribute to the reduction of edema.

More specifically, the MIRA technique regards the anatomical plane between the dermo-epidermal complex (DEC) and the superficial fascia. As part of the technique, the operator selects the most appropriate needle length and injection angle based on the patient's morphological characteristics as determined by ultrasound imaging (Table 1), to ensure extremely precise treatment, regardless of the technique used.

Table 1. Needle Selection and Injection Parameters.

Ultrasound parameters	Needle length	Injection depth & angle	Clinical rationale
Stage 3A	4–6 mm	Superficial injection at 30°–45°	Targets superficial adipose layer to reduce edema, improve skin turgor, and minimize unnecessary adipose removal
Stage 3B	13 mm	Deep bolus injection at 45°–90°	Acts on deep fibrous septae and excess adipose tissue, improves local drainage, reduces tissue rigidity
Stage Mixed	4–13 mm	30°–45°–90°	Targets overlapping or intermediate patterns adapting to the specificities of the tissues.

This personalized technique direct targets the adipocytes so that the volume of the adipocytes themselves is significantly reduced, contributing to a uniform and noticeable shrinkage of the fat lobules (Figure 1 A,B).

 doi:10.20944/preprints202603.0862.v1

A) 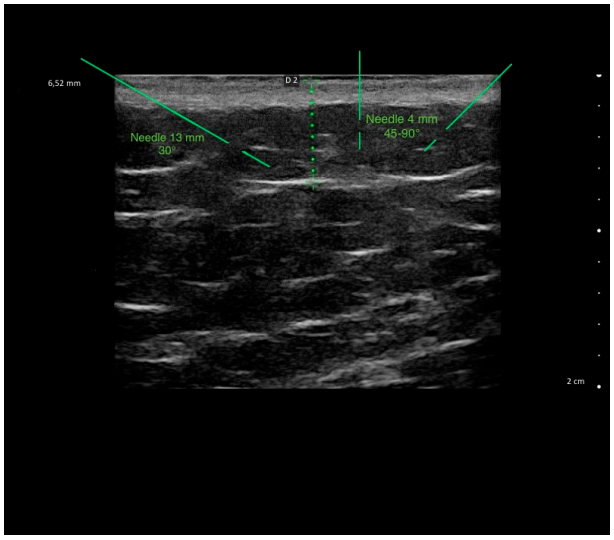

B) 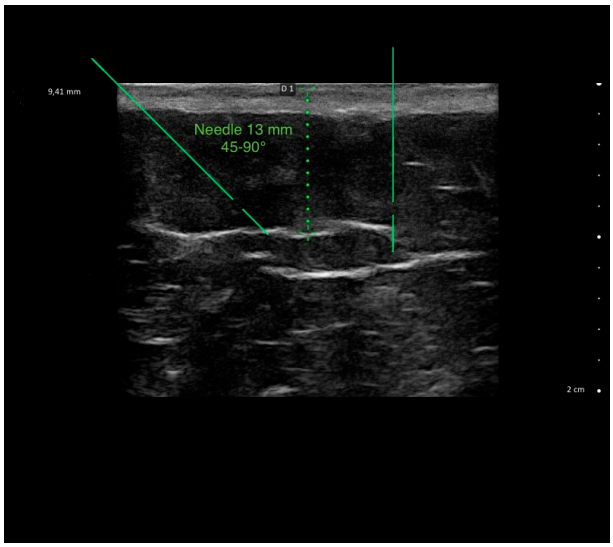

Figure 1. A–B. Ultrasound-guided PRI-INT protocol according to IEC staging. (A) Stage 3A – Mixed pattern: 13 mm needle at 30°, and 4–6 mm needle at 45° and 90°, adapting to moderate adipose thickness and mixed structural features. (B) Stage 3B: 13 mm needle at 45° and 90°, allowing deeper penetration for thick adipose panniculus and evident fibrous septa.

The progressive reduction in the size of the lobules significantly reduces the excessive mechanical stress on the fibrotic septa, which were thickened before treatment as an adaptive response to stabilize the connection between the DEC and the superficial fascia. The resulting relaxation initiates a dynamic remodeling process that allows the septa to gradually return to their physiological thickness and architecture and restore a more natural tissue organization. In addition, this structural adaptation reduces the compressive forces exerted by the enlarged adipocytes on the lobular vessels, resulting in a relevant improvement in local microcirculation. Key features of the MIRA technique compared to the standard techniques are shown in Table 2.

Table 2. Comparison between standard injection techniques and MIRA.

Aspect	Standard Technique	MIRA Technique
Needle selection	Fixed needle length, independent of patient anatomy	Needle length individualized according to ultrasound-derived subcutaneous thickness
Injection angle	Standardized angle (usually fixed for all patients)	Angle adapted to fascial integrity, fibrosis and edema as assessed by ultrasound
Treatment planning	Based on clinical staging only	Based on combined clinical and echographic staging (IEC system)
Targeting of tissue layers	Approximate, operator-dependent	Precise targeting of adipose lobules and fibrous septa identified on ultrasound
Reproducibility	High variability between operators	Reduced operator-dependent variability due to imaging-based guidance
Therapeutic goal	General improvement in skin appearance	Patient-specific correction of adipose hypertrophy, septal remodeling, edema reduction
Conceptual framework	Empirical aesthetic medicine	Precision aesthetic medicine, outcome-oriented

Patient Stratification and Treatment Technique

All patients underwent a standardized clinical and high-resolution ultrasound examination prior to treatment, as described by our research team in a recent study [21]. Based on a retrospective

 doi:10.20944/preprints202603.0862.v1

chart review, patients, treated with either CDT or IST according to cellulite stage severity, were assigned to MIRA groups (CDT_{MIRA} or IST_{MIRA}) or control groups (CDT_{CTL} or IST_{CTL}), depending on whether they received the MIRA technique.

In the MIRA groups, the operator selected the injection needle length and angle according to ultrasound parameters. In the control groups, no MIRA technique was applied: patients treated with Carbon Dioxide Therapy (CDT_{CTL}) systematically received a 13 mm needle, whereas those undergoing Injectable Solution Therapy (IST_{CTL}) systematically received a 4 mm needle, regardless of ultrasound findings.

Each participant included in the study completed six treatment sessions, administered at 15-day intervals.

Treatment Modalities

Both MIRA and control groups received the therapeutic modality determined by cellulite severity, classified according to the Nürnberger–Müller system. Patients with stage IIIA cellulite received carbon dioxide therapy (subcutaneous administration of medical CO_2), while those with stage IIIB cellulite underwent injectable solution therapy (a customized mixture of lipolytic and fibrolytic agents, vitamins, and peptides). After the treatment type (CDT or IST) was assigned based on staging, some patients underwent the MIRA technique, in which needle length and injection angle were tailored to ultrasound findings, while others received the same therapeutic modality using the standard fixed-needle technique (control groups).

Evaluation Methods

The assessment technique included objective imaging, clinical grading and patient-reported outcomes. High frequency ultrasound was used for IEC-based ultrasound staging, which allowed detailed assessment of subcutaneous tissue characteristics. Clinical grading was performed using the Nürnberger–Müller scale [22]. To ensure reproducibility, standardized photo documentation was created under identical lighting conditions, patient positioning and camera distance. Assessments were performed at baseline before treatment (T0) and 30 days after the end of the six treatment sessions (T1)

The primary outcome was change in ultrasound parameters, including thickness of adipose tissue, pain on palpation, presence of nodules, regularity of superficial fascia, cutaneous fibrosis, and edema. Secondary outcomes included patient satisfaction assessed using a visual analog scale (VAS 0-10), and assessment of visual appearance and skin side effects. The decision-making process applied for patients in the MIRA group is reported in Table 3.

Table 3. Schematic representation of **the** MIRA technique.

Step	Criteria / Actions
1. High-resolution ultrasound assessment	Subcutaneous thickness Fibrosis severity Edema grade Fascial integrity
2. Classification (IEC system)	Stage 3A Stage Mixed Stage 3B
3. Treatment type selection	Needle length selection: < 7.5 mm thickness → 4–6 mm needle > 7.5 mm thickness → 13 mm needle Injection angle selection: Superficial → 30°–45° Deep → 45°–90°

 doi:10.20944/preprints202603.0862.v1

4. MIRA guided injection procedure	Execution of the technique based on individualized parameters
5. Follow-up & outcome evaluation	Ultrasound assessment, clinical evaluation, and patient-reported satisfaction

Statistical Analysis

Continuous variables were expressed as mean (± standard deviation), median, and interquartile range, while categorical variables were presented as absolute frequencies and percentages. Changes from baseline (T0) to post-treatment (T1) and comparisons with controls were assessed separately for each treatment group (CDT or IST). For adipose tissue thickness, changes from T0 to T1 and between group (MIRA vs. CTL) were analyzed using mixed linear models with time and group as fixed effects, while age and BMI were included as covariates to adjust for potential confounding. For categorical outcomes, paired within-group comparisons between T0 and T1 were performed using McNemar's exact test for dichotomous variables and Stuart-Maxwell's test for categorial variables with more than two categories, whereas between-group comparisons (MIRA vs. CTL) at both time points were conducted using the Fisher's exact test. Patient-reported outcomes (satisfaction, perceived skin quality, and cellulite visual appearance) were summarized descriptively and compared using Mann-Whitney U test for continuous variables and Fisher's exact test for categorical variables. Analyses were conducted separately for the CDT and IST groups, without direct comparison between the two treatment modalities because of baseline severity differences among patients. This approach allowed both the comparison of each treatment arm with its respective control group and the assessment of pre–post changes within each arm while controlling for baseline differences in cellulite severity. To account for multiple testing, raw p-values were adjusted using the Benjamini–Hochberg false discovery rate (FDR) procedure, applied separately within each outcome domain. Adjusted p-values (p_{adj}) are reported alongside raw values, with statistical significance set at $p_{adj} \leq 0.05$. Statistical analyses were performed using STATA19 (StataCorp., College Station, TX, USA).

3. Results

A total of 120 patients were included in the study: 60 underwent treatment with the MIRA technique (30 with CDT_{MIRA} and 30 with IST_{MIRA}) and 60 were included in the control groups (30 CDT_{CTL} and 30 IST_{CTL}). Baseline demographic and clinical characteristics did not differ significantly between groups in terms of age, BMI, hormonal imbalances, or concomitant pharmacological therapies (Table 4).

Table 4. Baseline characteristics of patients.

	CDT_{MIRA}	**CDT_{CTL}**	**p-value**	**IST_{MIRA}**	**IST_{CTL}**	**p-value**
Age	37.1 (±9.6) [40, 30;43]	35.4 (±7.3) [33.5, 29;35.4]	0.425*	36.1 (±11) [33.5, 27;45]	35.9 (±10.3) [33.5, 27;45]	0.997*
BMI (kg/m2)	23.5 (±3.4) [22.5, 20.8;26.9]	22.9 (±2.3) [22.8, 20.9;22.9]	0.716*	24.3 (±3.3) [24.4, 21.4;27.2]	25 (±2.6) [25.25, 23.2;27.2]	0.447*
Hormonal Imbalances	0 (0.0)	2 (6.7)	0.492§	1 (3.3)	1 (3.3)	1.000§
Pharmacological therapies	1 (3.3)	2 (6.7)	1.000§	2 (6.7)	1 (3.3)	1.000§

Legend: Data are expressed as mean ± standard deviation and median [interquartile range] for continuous variables, and as absolute frequencies (percentages) for categorical variables. Comparisons between MIRA and

 doi:10.20944/preprints202603.0862.v1

control (CTL) groups were performed separately for carbon dioxide therapy (CDT) and injectable solution therapy (IST). * Mann–Whitney U test; § Fisher's exact test.

At follow-up 30 days after completion of the six treatment sessions, a significant reduction in subcutaneous adipose tissue thickness was observed in the MIRA groups (CDT_{MIRA}: from 6.7 ± 1.4 to 5.2 ± 1.1 mm, $p_{adj} = 0.002$; IST_{MIRA}: from 7.4 ± 1.5 to 5.6 ± 1.1 mm, $p_{adj} = 0.002$). In contrast, no significant changes were found in the control groups (CDT_{CTL}: from 6.9 ± 1.0 to 6.8 ± 0.9 mm; IST_{CTL}: from 7.1 ± 1.6 to 7.1 ± 1.5 mm). Between-group comparisons at follow-up confirmed highly significant differences in favor of MIRA (both $p_{adj} = 0.002$) (Table 5).

Table 5. Subcutaneous adipose tissue thickness at baseline (T0) and follow-up (T1).

	CDT_{MIRA}	CDT_{CTL}	p-value (p_{adj})	IST_{MIRA}	IST_{CTL}	p-value (p_{adj})
Baseline	6.7 (±1.4) [6.95, 5.3;7.9]	6.9 (±1.0) [6.85, 6.2;6.9]	0.343 (0.549)	7.4 (±1.5) [7.75, 6.7;8.5]	7.1 (±1.6) [7.65, 5.4;8.4]	0.843 (0.999)
Follow-up	5.2 (±1.1) [5.1, 4.5;6.2]	6.8 (±0.9) [6.8, 6.2;6.8]	<0.001 (0.002)	5.6 (±1.1) [5.55, 5.1;6.2]	7.1 (±1.5) [7.6, 5.4;8.1]	<0.001 (0.002)
p-value (p_{adj})	<0.001 (0.002)	0.993 (0.999)		<0.001 (0.002)	0.999 (0.999)	

Legend: Data are expressed as mean ± standard deviation and median [interquartile range]. Pre–post comparisons (T0 vs. T1) and between-group comparisons (MIRA vs. CTL) were performed using mixed linear models, adjusted for age and BMI as covariates.

The prevalence of pain decreased markedly in the MIRA groups (CDT_{MIRA}: from 60% to 23.3%, $p_{adj} = 0.003$; IST_{MIRA}: from 53.3% to 3.3%, $p_{adj} = 0.003$), while reductions were minor or absent in controls (CDT_{CTL}: from 80% to 66.7%, $p_{adj} = 0.072$; IST_{CTL}: unchanged at 53.3%, $p_{adj} = 1.000$). At follow-up, between-group comparisons revealed statistically significant differences in favor of MIRA compared with control (CDT: $p_{adj} = 0.005$; IST: $p_{adj} = 0.003$) (Table 6).

Table 6. Prevalence of pain on palpation at baseline (T0) and follow-up (T1).

	CDT_{MIRA}	CDT_{CTL}	p-value (p_{adj})	IST_{MIRA}	IST_{CTL}	p-value (p_{adj})
Baseline	18 (60.0)	24 (80.0)	0.158 (0.211)	16 (53.3)	16 (53.3)	1.000 (1.000)
Follow-up	7 (23.3)	20 (66.7)	0.002 (0.004)	1 (3.3)	16 (53.3)	<0.001 (0.003)
p-value (p_{adj})	0.001 (0.003)	0.045 (0.072)		<0.001 (0.003)	1.000 (1.000)	

Legend: Data are expressed as absolute numbers (percentages). Between-group comparisons (MIRA vs. CTL) at T0 and T1 were performed using the Fisher's exact test, while within-group pre–post comparisons (T0 vs. T1) were evaluated using the McNemar test.

The proportion of patients with nodules declined significantly in the MIRA groups (CDT_{MIRA}: from 63.3% to 23.3%, $p_{adj} = 0.003$; IST_{MIRA}: from 60% to 16.7%, $p_{adj} = 0.003$). In the control groups, only limited reductions were observed (CDT_{CTL}: from 83.3% to 66.7%, $p_{adj} = 0.040$; IST_{CTL}: from 73.3% to 66.7%, $p_{adj} = 0.179$). Post-treatment comparisons confirmed marked differences between MIRA and CTL (CDT: $p_{adj} = 0.004$; IST: $p_{adj} = 0.003$) (Table 7).

Table 7. Presence of subcutaneous nodules at baseline (T0) and follow-up (T1).

	CDT_{MIRA}	CDT_{CTL}	p-value (p_{adj})	IST_{MIRA}	IST_{CTL}	p-value (p_{adj})
Baseline	19 (63.3)	25 (83.3)	0.143	18 (60.0)	22 (73.3)	0.412

 doi:10.20944/preprints202603.0862.v1

			(0.179)			(0.412)
Follow-up	7 (23.3)	20 (66.7)	0.002 (0.004)	5 (16.7)	20 (66.7)	<0.001 (0.003)
p-value (p_{adj})	<0.001 (0.003)	0.025 (0.040)		<0.001 (0.003)	0.157 (0.179)	

Legend: Data are expressed as absolute numbers (percentages). Between-group comparisons (MIRA vs. CTL) at T0 and T1 were performed using the Fisher's exact test, while within-group pre–post comparisons (T0 vs. T1) were assessed using the McNemar test.

In the MIRA groups, the proportion of patients with regular fascia increased significantly (CDT_{MIRA}: from 66.7% to 86.7%, p_{adj} = 0.028; IST_{MIRA}: from 36.7% to 76.7%, p_{adj} = 0.008). In the control groups, fascia regularity remained unchanged or worsened (CDT_{CTL}: from 66.7% to 50.0%, p_{adj} = 0.154; IST_{CTL}: unchanged at 36.7%, p_{adj} = 1.000). At follow-up, MIRA showed clear improvements over controls (CDT: p_{adj} = 0.013; IST: p_{adj} = 0.013) (Table 8).

Table 8. Superficial fascia regularity at baseline (T0) and follow-up (T1).

	CDT_{MIRA}	**CDT_{CTL}**	**p-value (p_{adj})**	**IST_{MIRA}**	**IST_{CTL}**	**p-value (p_{adj})**
Baseline						
Regular	20 (66.7)	20 (66.7)	1.000 (1.000)	11 (36.7)	11 (36.7)	1.000 (1.000)
Irregular	10 (33.3)	10 (33.3)		19 (63.3)	19 (63.3)	
Follow-up						
Regular	26 (86.7)	15 (50.0)	0.005 (0.013)	23 (76.7)	11 (36.7)	0.004 (0.013)
Irregular	4 (13.3)	15 (50.0)		7 (23.3)	19 (63.3)	
p-value (p_{adj})	0.014 (0.028)	0.096 (0.154)		0.001 (0.008)	1.000 (1.000)	

Legend: Data are expressed as absolute numbers (percentages). Between-group comparisons (MIRA vs. CTL) at T0 and T1 were performed using the Fisher's exact test, while within-group pre–post comparisons (T0 vs. T1) were evaluated using the Stuart-Maxwell's test.

Edema prevalence decreased significantly in MIRA groups (CDT_{MIRA}: from 73.3% to 46.7%, p_{adj} = 0.016; IST_{MIRA}: from 90% to 63.3%, p_{adj} = 0.016), whereas in controls the improvement was not statistically significant (CDT_{CTL}: from 93.3% to 83.3%, p_{adj} = 0.111; IST_{CTL}: unchanged at 86.7%, p_{adj} = 1.000). Differences between MIRA and controls at follow-up were significant for CDT (p_{adj} = 0.016), but not for IST (p_{adj} = 0.111) (Table 9).

Table 9. Presence of edema at baseline (T0) and follow-up (T1).

	CDT_{MIRA}	**CDT_{CTL}**	**p-value (p_{adj})**	**IST_{MIRA}**	**IST_{CTL}**	**p-value (p_{adj})**
Baseline	22 (73.3)	28 (93.3)	0.080 (0.111)	27 (90.0)	26 (86.7)	1.000 (1.000)
Follow-up	14 (46.7)	25 (83.3)	0.006 (0.016)	19 (63.3)	26 (86.7)	0.072 (0.111)
p-value (p_{adj})	0.005 (0.016)	0.083 (0.111)		0.005 (0.016)	1.000 (1.000)	

Legend: Data are expressed as absolute numbers (percentages). Between-group comparisons (MIRA vs. CTL) at T0 and T1 were performed using the Fisher's exact test, while within-group pre–post comparisons (T0 vs. T1) were assessed using the McNemar test.

The prevalence of absent fibrosis increased substantially in the MIRA groups (CDT: from 13.3% to 43.3%, p_{adj} = 0.004; IST: from 16.7% to 36.7%, p_{adj} = 0.004), while controls showed no relevant

 doi:10.20944/preprints202603.0862.v1

improvements. Between-group comparisons confirmed a significant advantage for MIRA both in CDT (p_{adj} = 0.050) and IST (p_{adj} = 0.016) (Table 10).

Table 10. Cutaneous fibrosis at baseline (T0) and follow-up (T1).

	CDT_{MIRA}	CDT_{CTL}	p-value (p_{adj})	IST_{MIRA}	IST_{CTL}	p-value (p_{adj})
Baseline						
Absent	4 (13.3)	8 (26.7)		5 (16.7)	5 (16.7)	
Mild	16 (53.3)	12 (40.0)	0.586	5 (16.7)	6 (20.0)	1.000
Moderate	7 (23.3)	6 (20.0)	(0.938)	14 (46.7)	13 (43.3)	(1.000)
Grave	3 (10)	4 (13.3)		6 (20)	6 (20)	
Follow-up						
Absent	13 (43.3)	8 (26.7)		11 (36.7)	5 (16.7)	
Mild	16 (53.3)	12 (40.0)	0.025	13 (43.3)	7 (23.3)	0.006
Moderate	1 (3.3)	6 (20.0)	(0.050)	6 (20)	12 (40.0)	(0.016)
Grave	0 (0)	4 (13.3)		0 (0)	6 (20.0)	
p-value (p_{adj})	<0.001	1.000		<0.001	1.000	
(Baseline vs. Follow-up)	(0.004)	(1.000)		(0.004)	(1.000)	

Legend: Data are expressed as absolute numbers (percentages). Between-group comparisons (MIRA vs. CTL) at T0 and T1 were performed using the Fisher's exact test, while within-group pre–post comparisons (T0 vs. T1) were evaluated using the Stuart-Maxwell's test.

Consistent with the quantitative ultrasound findings, pre- and post-treatment images showed that the MIRA technique improved treatment precision within the affected areas, despite the heterogeneous morphological patterns of advanced cellulite among patients. After six treatment sessions, visible structural changes were evident in the regions previously identified and treated using the precision-guided MIRA approach (Figure 2). In contrast, similar improvements were not observed in the control groups, as reported in the Supplementary Materials (Figure S1).

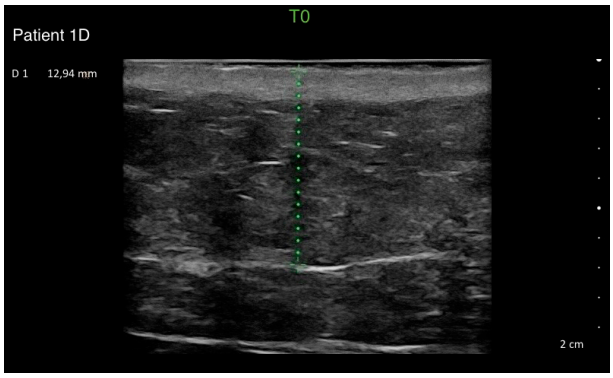

A)

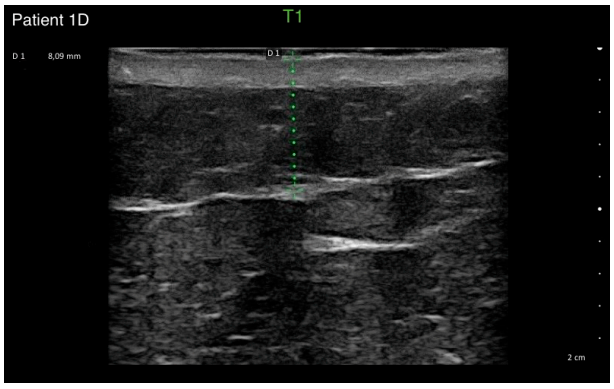

B)

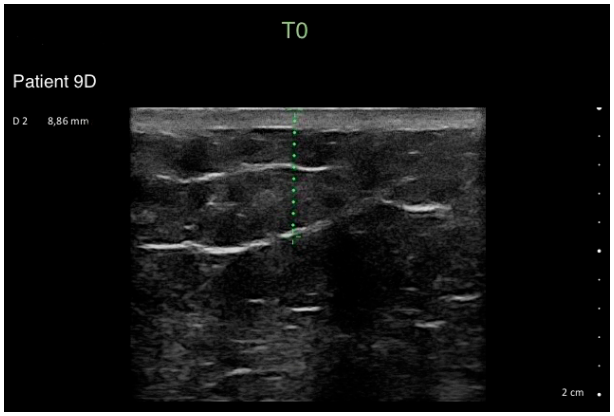

C)

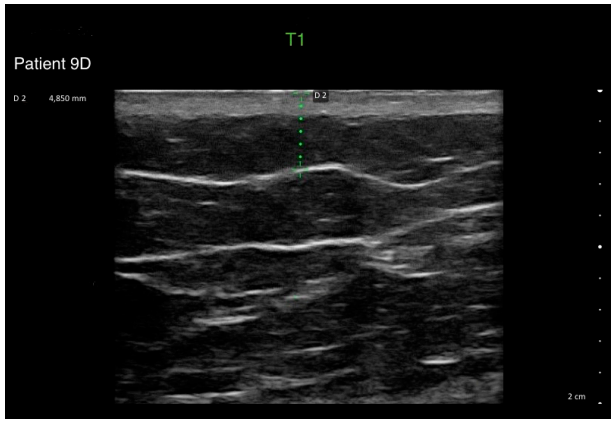

D)

 doi:10.20944/preprints202603.0862.v1

Figure 2. Representative ultrasound and external images of patients with stage 3 cellulite. (A) Baseline (T0) images of a patient with stage 3B cellulite and (B) corresponding post-treatment images after six MIRA sessions (T1), showing reduced adipose thickness and attenuation of fibrous septa. (C) Baseline (T0) images of a patient with mixed stage cellulite and (D) corresponding post-treatment images (T1), demonstrating decreased adipose layer and improved tissue architecture. Comparable improvements were not observed in the control groups (see Supplementary Materials).

Patient-reported satisfaction was significantly higher in the MIRA groups (CDT_{MIRA}: 8.1 ± 1.6; IST_{MIRA}: 8.5 ± 1.4) compared to controls (CDT_{CTL}: 6.1 ± 0.8; IST_{CTL}: 6.5 ± 0.7; both p_{adj} = 0.002). Improvement in skin quality was reported by 76.7% of CDT_{MIRA} and 83.3% of IST_{MIRA} patients, compared to only 13.3% and 20.0% in their respective controls (both p_{adj} = 0.002). Regarding cellulite visual appearance, absence of irregularities was observed in 63.3% of CDT_{MIRA} and 60% of IST_{MIRA} patients, compared with 3.3% and 16.7% in controls (both p_{adj} = 0.002) (Table 11).

Table 11. Patient-reported satisfaction, skin quality, and cellulite visual appearance at follow-up (T1).

	CDT_{MIRA}	CDT_{CTL}	p-value (p_{adj})	IST_{MIRA}	IST_{CTL}	p-value (p_{adj})
Perceived improvement	8.1 (±1.6) [8, 7;9]	6.1 (±0.8) [6, 6;6.1]	<0.001 (0.002)	8.5 (±1.4) [9, 8;10]	6.5 (±0.7) [6, 6;7]	<0.001 (0.002)
Skin quality						
As Before	3 (10.0)	19 (63.3)	<0.001 (0.002)	2 (6.7)	12 (40.0)	<0.001 (0.002)
Normal	4 (13.3)	7 (23.3)		3 (10.0)	12 (40.0)	
Improved	23 (76.7)	4 (13.3)		25 (83.3)	6 (20.0)	
Cellulite visual appearance T3						
Orange peel skin	5 (16.7)	19 (63.3)	<0.001 (0.002)	6 (20.0)	15 (50.0)	<0.001 (0.002)
Mild waviness	6 (20.0)	10 (33.3)		6 (20.0)	10 (33.3)	
Absent	19 (63.3)	1 (3.3)		18 (60.0)	5 (16.7)	

Legend: Satisfaction scores are expressed as mean ± standard deviation and median [interquartile range]. Skin quality and cellulite visual appearance are reported as absolute numbers (percentages). Between-group comparisons (MIRA vs. CTL) were performed using the Mann–Whitney U test for continuous variables and the Fisher's exact test for categorical variables.

4. Discussion

The main goal of this retrospective study was to evaluate the potential clinical utility of a novel image-guided technique for treating edematous fibrosclerotic panniculopathy. This technique, called Modulated Insertion of Regenerative Activation (MIRA), integrates high-resolution ultrasound into the treatment planning process to individualize key procedural parameters based on each patient's specific subcutaneous anatomy and pathological features.

Our findings indicate that the MIRA technique was associated with statistically significant and clinically relevant improvements. In each treatment group, paired pre–post analyses and between-group comparisons consistently showed reductions in subcutaneous adipose tissue thickness, palpable nodules, skin fibrosis, and interstitial edema, along with improved superficial fascial regularity and patient-reported skin appearance. These changes were not observed in the corresponding control groups, whose tissue architecture and ultrasound features remained largely unchanged after six sessions. Taken together, these results suggest that MIRA may enhance the effects of standard treatments (CDT or IST) by introducing an individualized approach that accounts for anatomical variability.

The rationale for MIRA aligns with the current understanding of cellulite pathophysiology, in which changes at the dermo-hypodermal junction, microcirculatory disturbances, and disorganization of adipose tissue architecture play a central role. Injectable approaches that

 doi:10.20944/preprints202603.0862.v1

simultaneously target adipose hypertrophy and fibrous septal remodeling have demonstrated synergistic effects in improving surface irregularities[11]. Consistent with this evidence, our results support previous studies highlighting the therapeutic potential of injection-based interventions for cellulite[13,14,18], while introducing the innovative element of systematically integrating ultrasound guidance to tailor treatment parameters. Additionally, recent studies have emphasized that multimodal strategies generally produce better and longer-lasting improvements in cellulite severity compared with monothetic techniques[11,23]. This evidence supports the MIRA concept, which combines imaging-guided diagnosis, personalized parameter selection, and precise execution within a unified therapeutic framework.

From a mechanistic standpoint, the reduction in subcutaneous adipose tissue thickness and interstitial edema observed with MIRA may plausibly be explained by improved microcirculation and lymphatic drainage achieved through accurate targeting of the affected layers[24,25]. These changes are clinically relevant, as pannicle thickness correlates directly with the degree of visible dimpling and contour irregularities. By mapping tissue layers and adapting needle length and injection angle to each anatomical pattern, MIRA may optimize treatment delivery and achieve measurable reductions in adipose hypertrophy, with corresponding improvements in both objective measures and patient-reported outcomes[8]. In parallel, the attenuation of fibrosis and improvement in fascial regularity may result from ultrasound-guided control of injection depth and angle, which facilitates direct remodeling of pathological fibrous septa. Restoration of continuity, tensile strength, and elasticity of the superficial fascial system is a therapeutic target, given that fascial discontinuity contributes to the protrusion of subcutaneous fat lobules into the dermis and the characteristic “orange peel” appearance[22,26]. The more pronounced improvement in fascial architecture observed in the carbon dioxide therapy group is consistent with the MIRA principle of addressing multiple pathophysiological processes simultaneously. This interpretation is further supported by recent findings showing that restoration of fascial organization reduces the herniation of fat lobules and contributes to smoother surface contours[27]. Although we did not directly measure microcirculatory or lymphatic changes, the ultrasound-based improvements suggest that these mechanisms may contribute to the observed outcomes.

Finally, the integrated effect of MIRA, combining ultrasound-based diagnostic targeting, optimized needle placement, and either CO_2-induced metabolic activation or pharmacological mixtures, may account for the simultaneous reduction of fibrosis, edema, and pannicular disorganization. Through progressive septal normalization, mobilization of interstitial fluid, and improved tissue compliance, this multimodal approach provides a plausible mechanistic basis for the structural remodeling and improvements in tissue architecture documented in this study[28,29].

MIRA may represent a refinement of traditional injection-based modalities by integrating high-resolution ultrasound as a decision-support tool in the treatment process. Within this framework, MIRA exemplifies the emerging field of precision esthetic medicine, where diagnostic imaging and tailored procedural parameters are combined to enable patient-specific and potentially more reproducible interventions. This integration allows the operator to adjust key technical parameters according to the patient’s individual anatomy and pathological features, including subcutaneous adipose thickness, fibrous septal organization, interstitial edema, and fascial integrity[7,19]. Such individualized planning enables precise delivery of treatments to the intended tissue compartment, thereby enhancing the impact on the pathological substrate. By ensuring more homogeneous interaction with the target structures, this approach may improve the remodeling of fibrous septa and the pharmacological or metabolic effects of the injected substances. Moreover, ultrasound-guided parameter selection may help mitigate operator-dependent variability, a recognized limitation of traditional non-guided techniques[21], and thus contribute to improved reproducibility, longer-lasting results, and overall treatment quality[8].

Recent anatomical studies further support the MIRA framework. The three-dimensional model of the subdermal septal system described by Cotofana and Kaminer (2022) highlights the dynamic architecture of the retinacula cutis, superficial fascia, and fat lobules, as well as sex-specific differences

 doi:10.20944/preprints202603.0862.v1

in connective tissue organization[30]. This updated perspective underscores the structural complexity of cellulite and reinforces the rationale for imaging-based, anatomy-guided techniques. By adapting injection parameters to ultrasound assessments of these structures, MIRA directly addresses the morpho-functional heterogeneity of the subcutaneous compartment and bridges the gap between contemporary anatomical insights and therapeutic application.

This study has some limitations. Its retrospective design may have introduced selection bias and precludes causal inference. Because of this design, no a priori sample size calculation was performed; instead, all eligible cases during the study period were included, which ensured completeness but may have limited statistical power, particularly in subgroup analyses. The short follow-up period (30 days) does not allow evaluation of long-term durability, and mechanistic interpretations remain speculative, as microcirculatory and lymphatic changes were not directly measured.

5. Conclusions

This retrospective study suggests that MIRA may be associated with structural and esthetic improvements in advanced cellulite. By integrating high-resolution imaging into procedure planning, MIRA combines diagnostic assessment with therapeutic execution and may help reduce operator-dependent variability. Larger, prospective, randomized clinical trials with validated clinical scales and longer follow-up are needed to confirm efficacy and assess durability. In this context, MIRA could eventually serve not only as a therapeutic option but also as a decision-support framework in esthetic medicine, consistent with the principles of precision approaches.

Supplementary Materials: The following supporting information can be downloaded at the website of this paper posted on Preprints.org, Figure S1. Representative ultrasound and external images of control patients with stage 3 cellulite. (A) Baseline (T0) images of a patient treated with CDT and (B) corresponding post-treatment images after six sessions (T1), showing no relevant changes in adipose thickness or fibrous septa. (C) Baseline (T0) images of a patient treated with IST and (D) corresponding post-treatment images (T1), similarly demonstrating persistence of adipose layer and unchanged tissue architecture.

Author Contributions: The authors contributed equally to this work.

Funding: This research received no external funding.

Institutional Review Board Statement: Ethical review and approval were waived for this study because all procedures were part of routine clinical practice in aesthetic medicine and were performed exclusively using CE-marked medical devices within their approved indications, without the introduction of investigational drugs, devices, or experimental interventions. The study did not involve any deviation from standard care pathways and was classified as a methodological/quality improvement evaluation of routine practice in accordance with Italian regulations (Ministerial Decree of 2 September 2002 and subsequent AIFA updates), which do not consider such activities as clinical trials. The waiver was formally granted by the Clinical Medical Directorate (Prot. 04/2024).

Informed Consent Statement: Informed consent was obtained from all subjects involved in the study.

Data Availability Statement: The data supporting the findings of this study are available from the corresponding author upon reasonable request, subject to compliance with applicable privacy regulations and the General Data Protection Regulation (GDPR), and institutional data protection policies.

Conflicts of Interest: The authors declare no conflicts of interest.

Abbreviations

The following abbreviations are used in this manuscript:

CDT	Carbon Dioxide Therapy
DEC	Dermo-Epidermal Complex
EFP	Edematous Fibrosclerotic Panniculopathy

 doi:10.20944/preprints202603.0862.v1

IST	Injectable Solution Therapy
MIRA	Modulated Insertion of Regenerative Activation

References

1. Sfyri, E. Cellulite – Etiology, Epidemiology and Management. **2025**, *39*, 25-28, doi:10.61873/vhxh4395.
2. Tanzi, E.L.; Capelli, C.C.; Robertson, D.W.; LaTowsky, B.; Balcom-Luker, S.; Jacob, C.; Ibrahim, O.; Kaminer, M.S. Improvement in Cellulite Appearance After a Single Treatment Visit With Acoustic Subcision: Long-Term Findings From a Multicenter Clinical Trial. *Dermatol Surg* **2023**, *50*, 165-170, doi:10.1097/dss.0000000000004000.
3. Bass, L.S.; Hibler, B.P.; Khalifian, S.; Shridharani, S.M.; Klibanov, O.M.; Moradi, A. Cellulite Pathophysiology and Psychosocial Implications. *Clin Cosmet Investig Dermatol.* **2023**, *49*, S2-S7, doi:10.1097/dss.0000000000003745.
4. Hartman, N.; Almukhtar, R.; Wood, E.S.; Fabi, S.G. Collagenase Clostridium Histolyticum-Aaes Injections for Volumetric Change of Cellulite Dimples and Gluteal Contouring. *Dermatol Surg* **2023**, *49*, 383-386, doi:10.1097/dss.0000000000003727.
5. Nobile, V.; Cestone, E.; Puoci, F.; Ponti, I.D.; Pisati, M.; Michelotti, A. In Vitro and in Vivo Study on Humans of Natural Compound Synergy as a Multifunctional Approach to Cellulite-Derived Skin Imperfections. *Cosmetics* **2020**, *7*, 48, doi:10.3390/cosmetics7020048.
6. Bennardo, L.; Fusco, I.; Cuciti, C.; Sicilia, C.; Salsi, B.; Cannarozzo, G.; Hoffmann, K.; Nisticò, S.P. Microwave Therapy for Cellulite: An Effective Non-Invasive Treatment. *J Clin Med* **2022**, *11*, 515, doi:10.3390/jcm11030515.
7. Mlosek, K.; Malinowska, S. High-Frequency Ultrasound in the Assessment of Cellulite—Correlation Between Ultrasound-Derived Measurements, Clinical Assessment, and Nürnberger–Müller Scale Scores. *Diagnostics* **2024**, *14*, 1878, doi:10.3390/diagnostics14171878.
8. Sadick, N.S.; Goldman, M.P.; Liu, G.; Shusterman, N.H.; McLane, M.; Hurley, D.; Young, V.L. Collagenase Clostridium Histolyticum for the Treatment of Edematous Fibrosclerotic Panniculopathy (Cellulite): A Randomized Trial. *Dermatol Surg* **2019**, *45*, 1047-1056, doi:10.1097/dss.0000000000001803.
9. Sant'Ana, E.M.C.; Pianez, L.R.G.; Custódio, F.S.; Guidi, R.M.; Freitas, J.N.d. Effectiveness of Carboxytherapy in the Treatment of Cellulite in Healthy Women: A Pilot Study. *Clin Cosmet Investig Dermatol.* **2016**, *Volume 9*, 183-190, doi:10.2147/ccid.s102503.
10. Di Guardo, A.; Solito, C.; Cantisani, V.; Rega, F.; Gargano, L.; Rossi, G.; Musolff, N.; Azzella, G.; Paolino, G.; Losco, L.; et al. Clinical and Ultrasound Efficacy of Topical Hypertonic Cream (Jovita Osmocell(®)) in the Treatment of Cellulite: A Prospective, Monocentric, Double-Blind, Placebo-Controlled Study. *Medicina (Kaunas)* **2024**, *60*, doi:10.3390/medicina60050781.
11. Pérez Atamoros, F.M.; Alcalá Pérez, D.; Asz Sigall, D.; Ávila Romay, A.A.; Barba Gastelum, J.A.; de la Peña Salcedo, J.A.; Escalante Salgado, P.E.; Gallardo Palacios, G.J.; Guerrero-Gonzalez, G.A.; Morales De la Cerda, R.; et al. Evidence-based treatment for gynoid lipodystrophy: A review of the recent literature. *J Cosmet Dermatol* **2018**, *17*, 977-983, doi:10.1111/jocd.12555.
12. Bagherani, N.; Smoller, B.R.; Tavoosidana, G.; Ghanadan, A.; Wollina, U.; Lotti, T. An Overview of the Role of Carboxytherapy in Dermatology. *J Cosmet Dermatol* **2023**, *22*, 2399-2407, doi:10.1111/jocd.15741.
13. Chieregato, F.; Silva, C.N.d.; Carvalho, T.M.D.; Grecco, C.; Moreira, R.G.; Guidi, R.M.; Girola, L.F.; Souza, J.R.d.; Modena, D.A.O. Effects of Multi-Directional Oscillatory Vibration in the Treatment of Cellulite and Body Remodeling. *Fisioterapia Brasil* **2020**, *21*, 77-85, doi:10.33233/fb.v21i1.2820.
14. Melo, D.F.; Barreto, T.d.M.; Plata, G.T.; Araujo, L.R.; Tortelly, V.D. Excellent Response to Mesotherapy as Adjunctive Treatment in Male Androgenetic Alopecia. *J Cosmet Dermatol* **2019**, *19*, 75-77, doi:10.1111/jocd.12983.
15. Podgórna, K.; Kołodziejczak, A.; Rotsztejn, H. Cutometric Assessment of Elasticity of Skin With Striae Distensae Following Carboxytherapy. *J Cosmet Dermatol* **2017**, *17*, 1170-1174, doi:10.1111/jocd.12465.
16. Kołodziejczak, A.; Jatczak, A.; Rotsztejn, H. The Correlation Between the Severity of Symptoms and the Thickness of the Fat Fold in Cellulite-affected Areas—A Pilot Study. *J Cosmet Dermatol* **2022**, *21*, 5852-5858, doi:10.1111/jocd.15129.

 doi:10.20944/preprints202603.0862.v1

17. Tang, Z.; Hu, Y.; Wang, J.; Fan, Z.; Qu, Q.; Miao, Y. Current Application of Mesotherapy in Pattern Hair Loss: A systematic Review. *J Cosmet Dermatol* **2022**, *21*, 4184-4193, doi:10.1111/jocd.14900.
18. Eldsouky, F.; Ebrahim, H.M. Evaluation and Efficacy of Carbon Dioxide Therapy (Carboxytherapy) Versus Mesolipolysis in the Treatment of Cellulite. *Journal of Cosmetic and Laser Therapy* **2018**, *20*, 307-312, doi:10.1080/14764172.2017.1400175.
19. Bauer, J.; Grabarek, M.; Migasiewicz, A.; Podbielska, H. Non-Contact Thermal Imaging as Potential Tool for Personalized Diagnosis and Prevention of Cellulite. *J Therm Anal Calorim* **2018**, *133*, 571-578, doi:10.1007/s10973-018-7232-9.
20. Intagliata, D.; Garo, M.L. The Role of Ultrasound in the Diagnosis and Treatment of Cellulite: A Systematic Review. *J Clin Med* **2026**, *15*, 943, doi:10.3390/jcm15030943.
21. Intagliata, D.; Priolo, M.; Molinari, P. High-Frequency Ultrasound Imaging for Stage III Cellulite: A Three-Subtype Structural Classification from an Observational Cohort Study. *Dermatology and Therapy* **2025**, doi:10.1007/s13555-025-01504-0.
22. Nürnberger, F.; Müller, G. So-Called Cellulite: An Invented Disease. *J Dermatol Surg* **1978**, *4*, 221-229, doi:https://doi.org/10.1111/j.1524-4725.1978.tb00416.x.
23. Dal'Forno, T.; Del Nero, M.P.; Nunes, F.; Cunha, C.; Haddad, A.; Vilarinho, A.; Nogueira, A.; Tomaz, R. Recomendações clínicas para o uso combinado de ácido poli-L-láctico (PLLA-SCA) e dispositivos baseados em energia: opinião de especialistas e revisão da literatura. *Surgical & Cosmetic Dermatology* **2025**, *17*, 1-10, doi:10.5935/scd1984-8773.2025170377.
24. Gabriel, A.; Chan, V.; Caldarella, M.; Wayne, T.; O'Rorke, E. Cellulite: Current Understanding and Treatment. *Aesthet Surg J Open Forum* **2023**, *5*, ojad050, doi:10.1093/asjof/ojad050.
25. Hexsel, D.M.; Siega, C.; Schilling-Souza, J.; Porto, M.D.; Rodrigues, T.C. A bipolar radiofrequency, infrared, vacuum and mechanical massage device for treatment of cellulite: a pilot study. *J Cosmet Laser Ther* **2011**, *13*, 297-302, doi:10.3109/14764172.2011.630086.
26. Querleux, B.; Cornillon, C.; Jolivet, O.; Bittoun, J. Anatomy and physiology of subcutaneous adipose tissue by in vivo magnetic resonance imaging and spectroscopy: relationships with sex and presence of cellulite. *Skin Res Technol* **2002**, *8*, 118-124, doi:10.1034/j.1600-0846.2002.00331.x.
27. Fede, C.; Clair, C.; Pirri, C.; Petrelli, L.; Zhao, X.; Sun, Y.; Macchi, V.; Stecco, C. The Human Superficial Fascia: A Narrative Review. *Int J Mol Sci* **2025**, *26*, 1289.
28. Rossi, A.B.R.; Vergnanini, A.L. Cellulite: a review. *J Eur Acad Dermatol Venereol* **2000**, *14*, 251-262, doi:https://doi.org/10.1046/j.1468-3083.2000.00016.x.
29. Terranova, F.; Berardesca, E.; Maibach, H. Cellulite: nature and aetiopathogenesis. *International Journal of Cosmetic Science* **2006**, *28*, 157-167, doi:https://doi.org/10.1111/j.1467-2494.2006.00316.x.
30. Cotofana, S.; Kaminer, M.S. Anatomic update on the 3-dimensionality of the subdermal septum and its relevance for the pathophysiology of cellulite. *J Cosmet Dermatol* **2022**, *21*, 3232-3239, doi:10.1111/jocd.15087.